Supplementary Information (SI) for Nanoscale.
This journal is © The Royal Society of Chemistry 2025

Pressure effects on the surface enhanced Raman spectroscopy of ZIF-67/R6G system

K. Kamali[a*], K. A. Irshad[b], Muthukumaran Sundaramoorthy[b], Boby Joseph[b] and Dipti. P. Das[a]

[a] CSIR-Institute of Minerals and Materials Technology, Odisha, India

[b] Elettra - Sincrotrone Trieste S.C. p. A., S.S. 14, Km 163.5 in Area Science Park, Basovizza 34149, Italy

*Email: kamalikesavan@immt.res.in

Experimental details

2.1. Materials

$Co(NO_3)_2 \cdot 6H_2O$ (99%) and 2-methylimidazole (98%) were procured from Hi Media and TCI. Rhodamine 6G (90+%) was procured from Alfa Aesar. All the reagents used in the experiment were of analytical grade and used without further purification.

2.2. Synthesis and characterisation

The synthesis procedure of ZIF-67 was followed as in the earlier report with little modification [1]. $Co(NO_3)_2 \cdot 6H_2O$ (1.64 g) was dissolved in 80 mL of methanol, and then a mixture of 2-methylimidazole (3.70 g) with 80 mL of methanol was added to the above solution under vigorous stirring for 24 h. Finally, the purple product precipitates formed at the end of the reaction were collected by centrifugation (7000 rpm for 20 min), washed several times with methanol, and dried at 60 °C for 6 hrs. Before use, the samples were redried at 100 °C under vacuum for 5 h. The phase identity and purity of ZIF-67 were determined by X-ray powder diffraction (XRPD) using synchrotron radiation with the wavelength $\lambda = 0.4957$ Å, at the Xpress beamline of the Elettra Synchrotron, Trieste [2]. XPS measurements were performed on a K-Alpha$^+$ X-Ray photo electron spectrometer with Al Kα (monochromatic) with 6 mA beam current & 12 KV as the x-ray radiation source and spot size 400 µm. The UV-Vis diffuse reflectance spectra of powder samples were recorded with Cary 100, Agilent spectrophotometer. UV-DRS were used to obtain the information on the optical properties and energy band structure of the samples. The surface morphology was characterized by FESEM (CARL ZEISS, SUPRA55). Transmission electron microscopy (TEM) investigation was carried out using a JEOL-JEM F 200 TEM operated at 200 kV. Photoluminescence (PL) measurements were performed using a Renishaw Raman Spectrometer with an excitation wavelength of 532 nm. The pore properties were analyzed from N_2 adsorption-desorption isotherms obtained at 77 K using an adsorption apparatus ASAP 2020 (Micromeritics, USA). The pore size distribution curves were calculated from the desorption branch of the nitrogen isotherm by the HK (Figure S6). Prior to analysis, the sample was degassed at 100 ^{o}C under a vacuum.

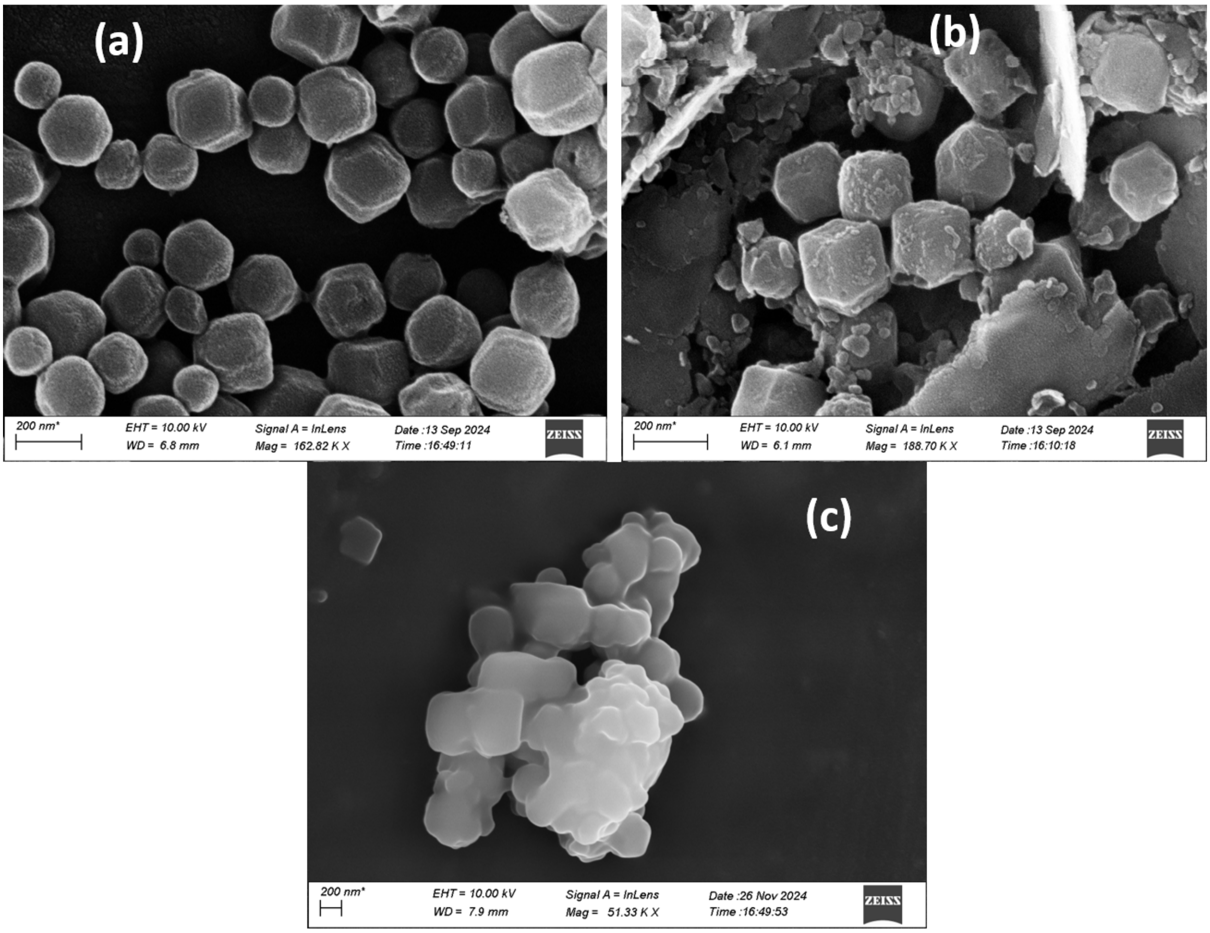

Figure S1. Field Emission Scanning Electron Microscopy (FESEM) image of synthesised pristine ZIF-67 (a) ZIF-67/R6G (b) hand-ground morphology of ZIF-67/R6G (c).

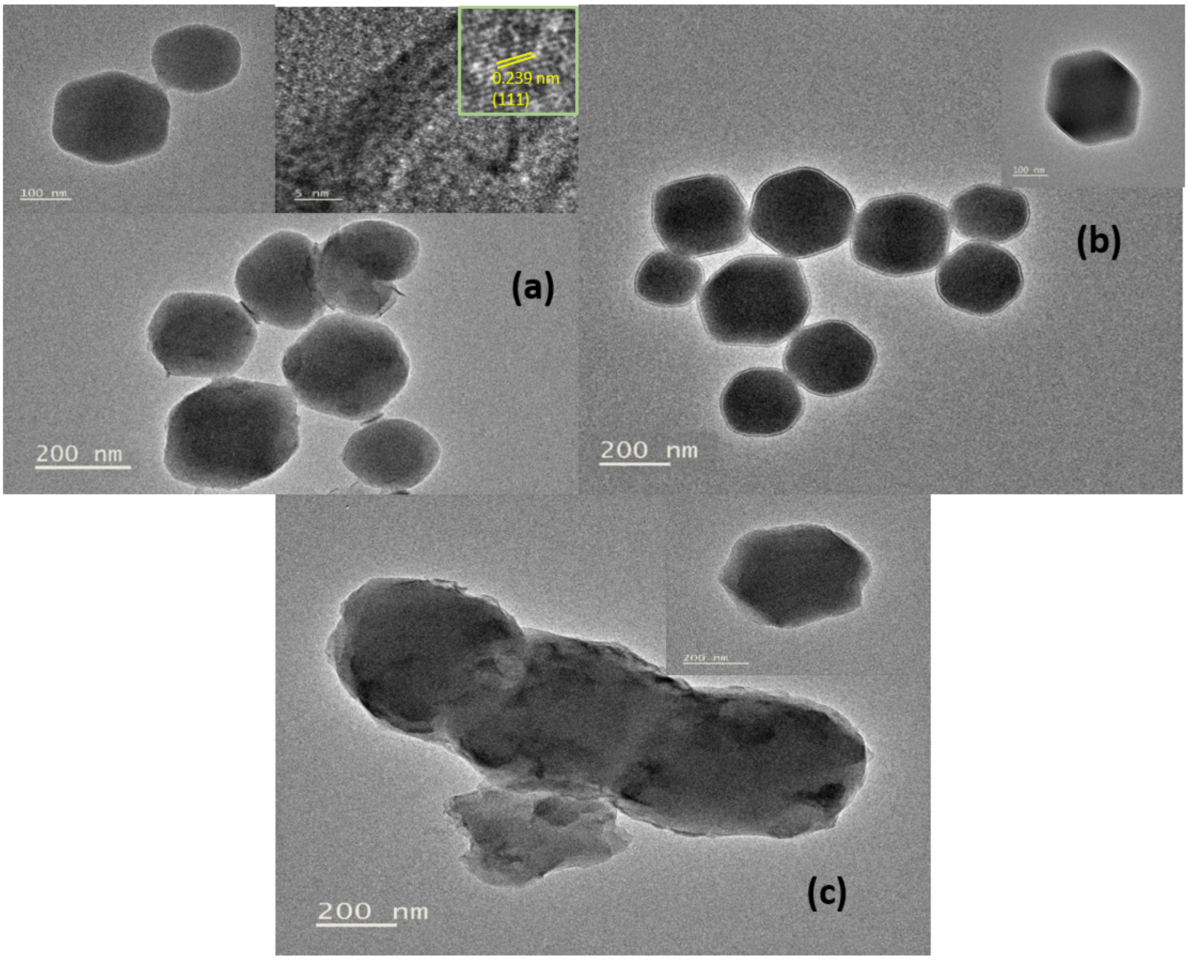

Figure S2. TEM images of (a) pristine ZIF-67 at 200 nm scale (inset shows the TEM image at 100 nm scale and HRTEM image at 5 nm scale with lattice plane of (111)) (b) ZIF-67/R6G with inset of 100 nm scale and (c) Ground ZIF-67/R6G of irregular morphology with distorted single particle in inset.

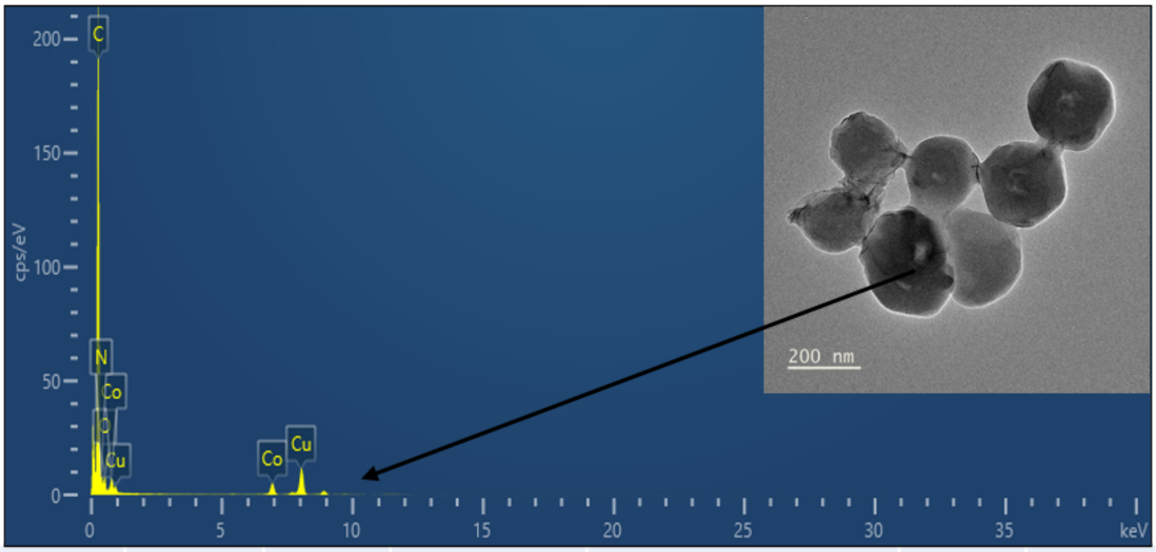

Element	Line Type	k Factor	k Factor type	Absorption Correction	Wt%	Wt% Sigma
C	K series	3.115	Theoretical	1	88.61	0.14
N	K series	1.807	Theoretical	1	2.9	0.12
O	K series	1.455	Theoretical	1	1.51	0.05
Co	K series	1.286	Theoretical	1	1.84	0.04
Cu	K series	1.421	Theoretical	1	5.13	0.06
Total:					100	

Figure S3. STEM image of pristine ZIF-67 drop-cast on copper grid (inset), together with the EDX spectra. Elemental concentrations estimated from the EDX is shown below in the table.

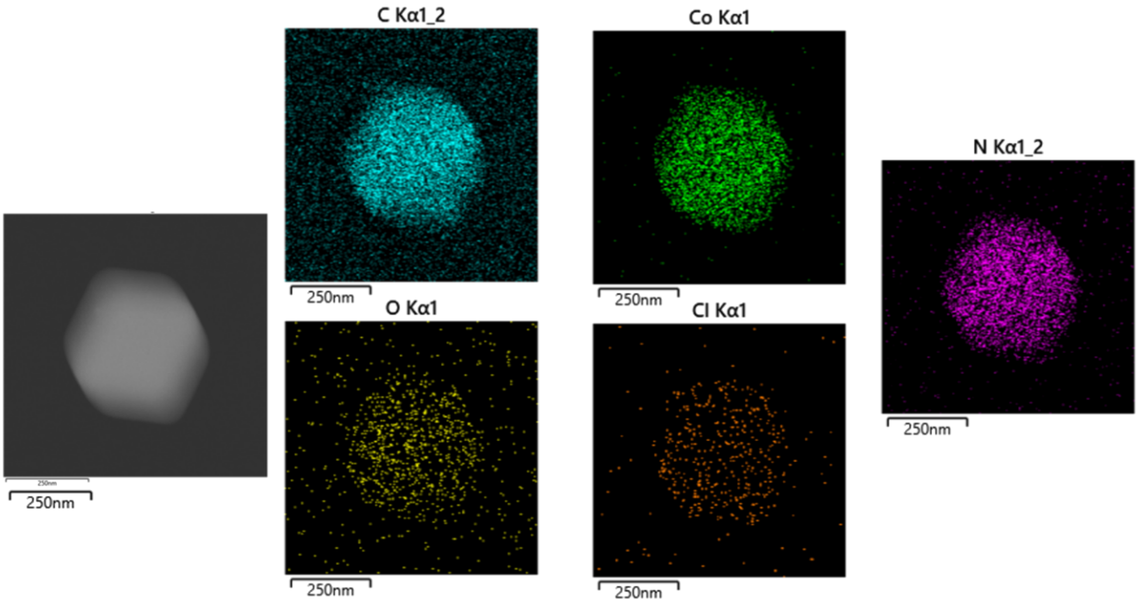

Figure S4. Element mapping of ZIF-67/R6G showing the phase purity and homogeneous distribution of different elements throughout the sample. Element chlorine is from R6G analyte molecule.

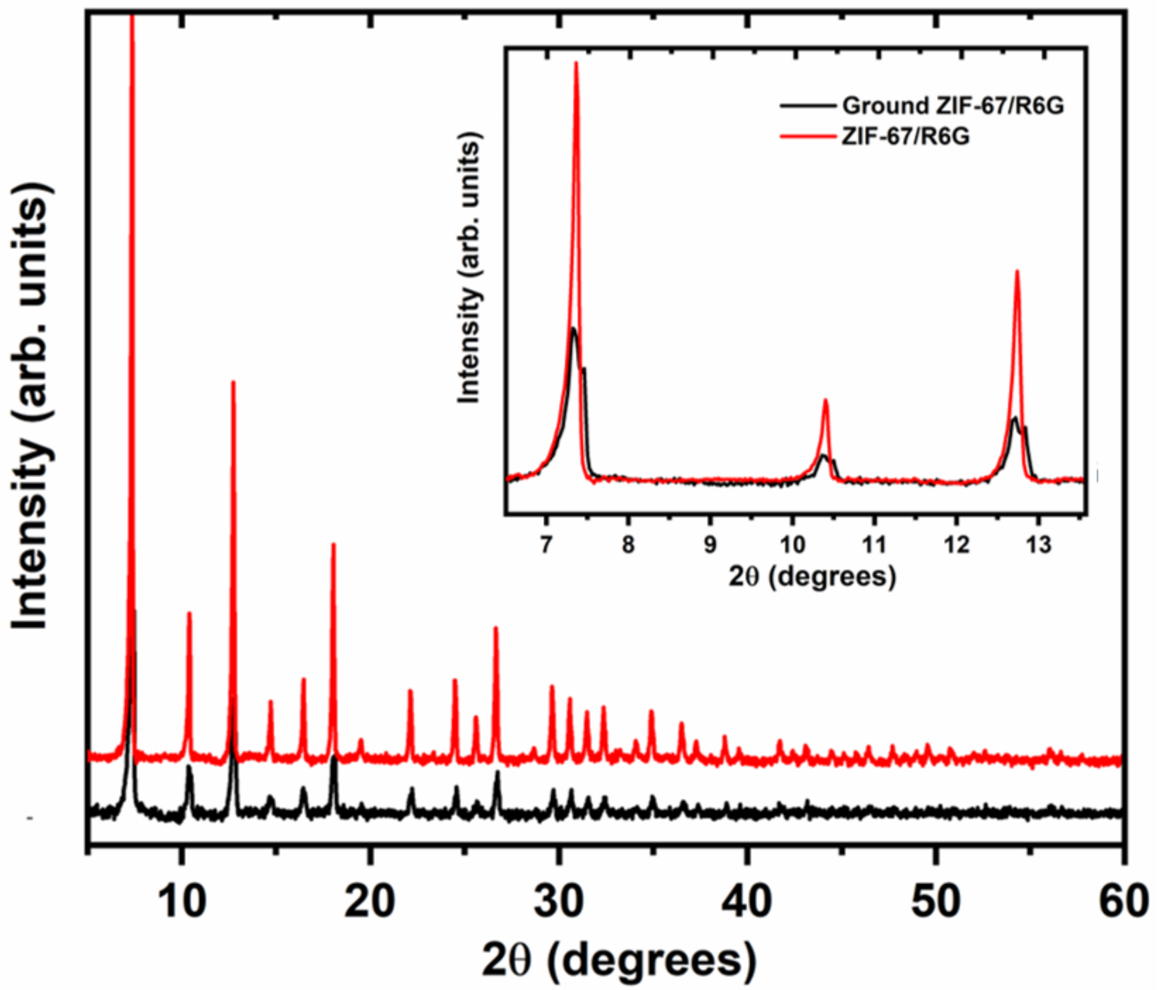

Figure S5. Comparison of XRD patterns of ZIF-67/R6G and hand ground ZIF-67/R6G recorded with Cu Kα source with a wavelength of 1.54 Å at ambient conditions.

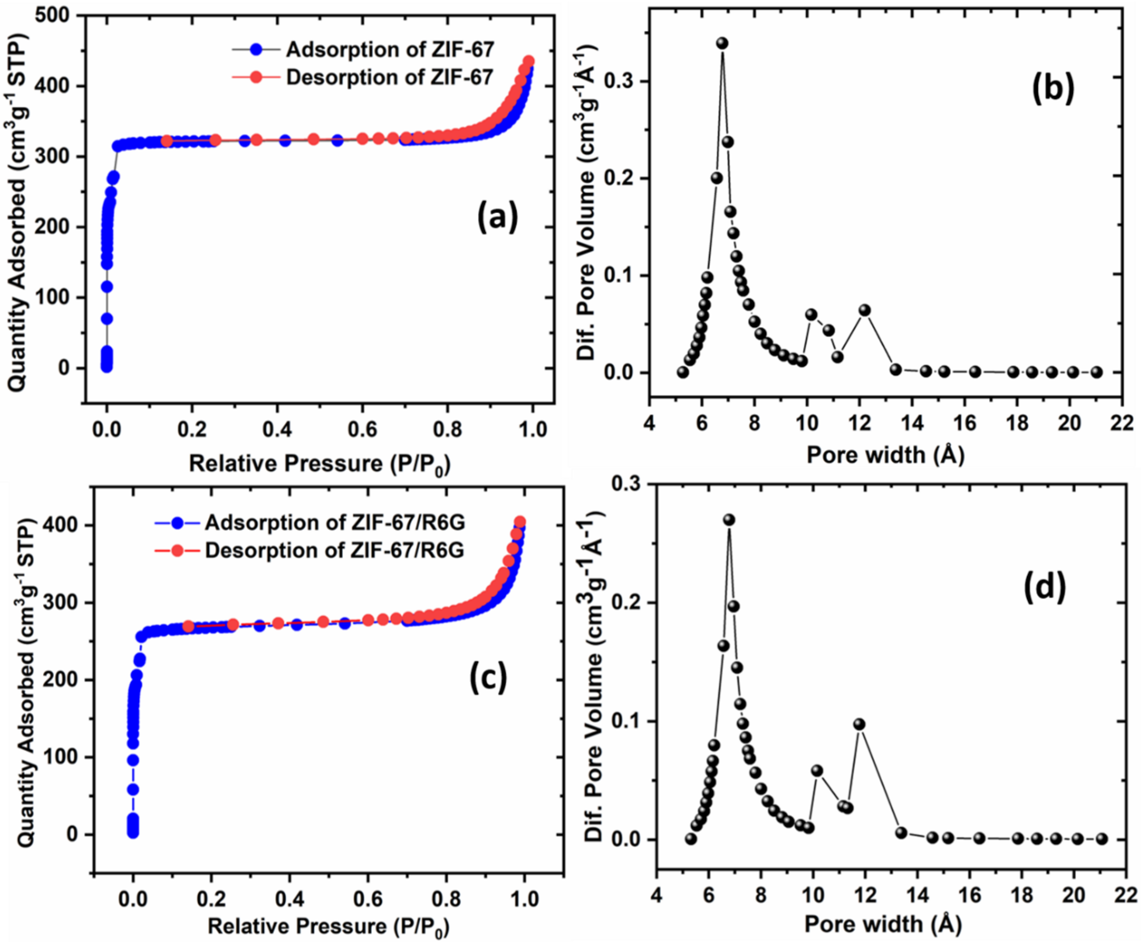

Figure S6. (a and b) N_2 adsorption-desorption isotherm at 77 K and pore size distribution of pristine ZIF-67 (c and d) N_2 adsorption-desorption isotherm at 77 K and pore size distribution of ground ZIF-67/R6G demonstrate a reduction in the surface area.

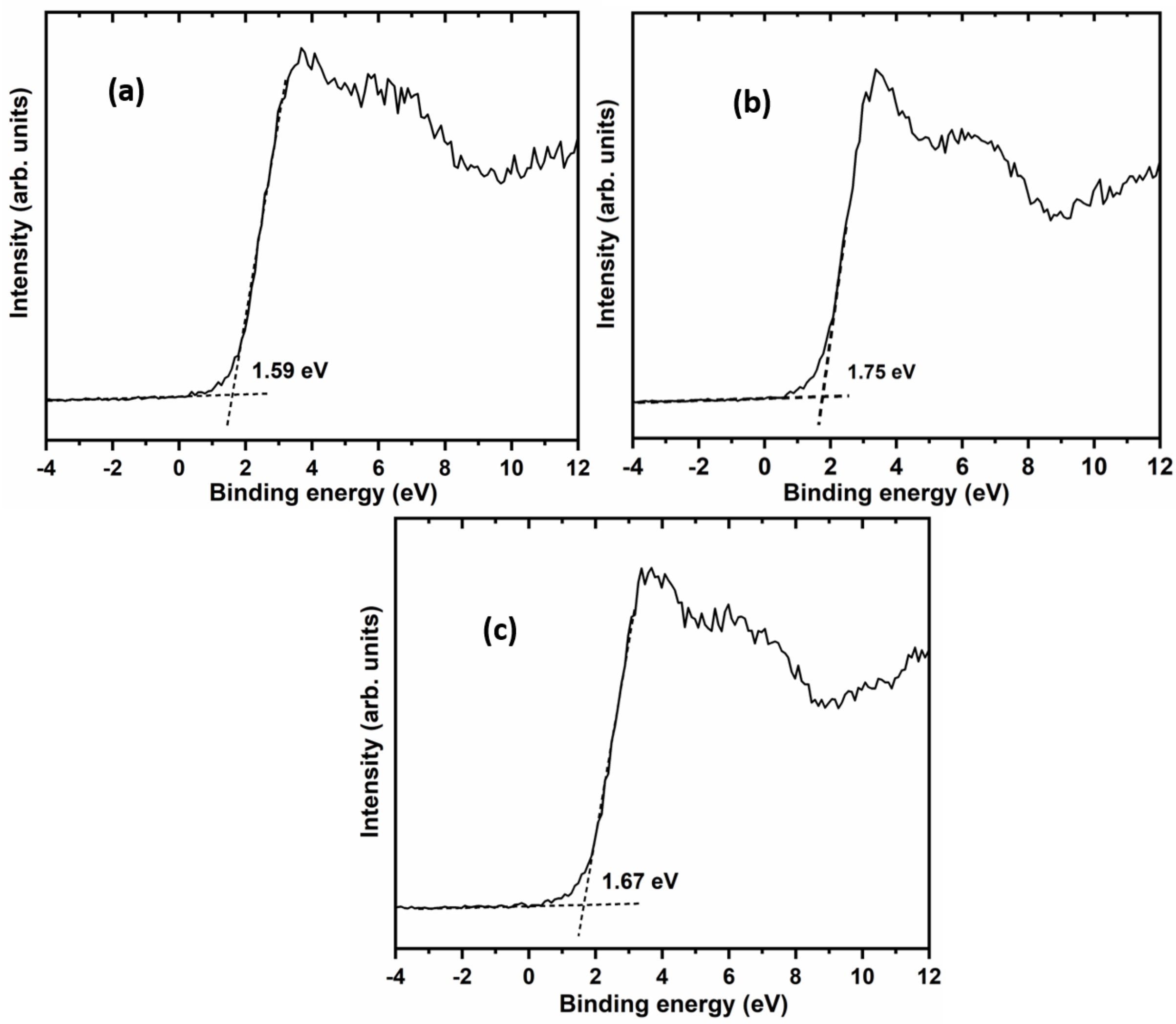

Figure S7 **(a)**Valence-band XPS spectrum of pristine ZIF-67 **(b)** ZIF-67/R6G and **(c)** ground ZIF-67/R6G.The HOMO position of all the samples are determined by linear extrapolation of the leading edges of the profile to the baseline [1]. After calibration with the reference Fermi level, The HOMO value for ZIF-67 is calculated to be 6.40 eV with respect to vacuum.

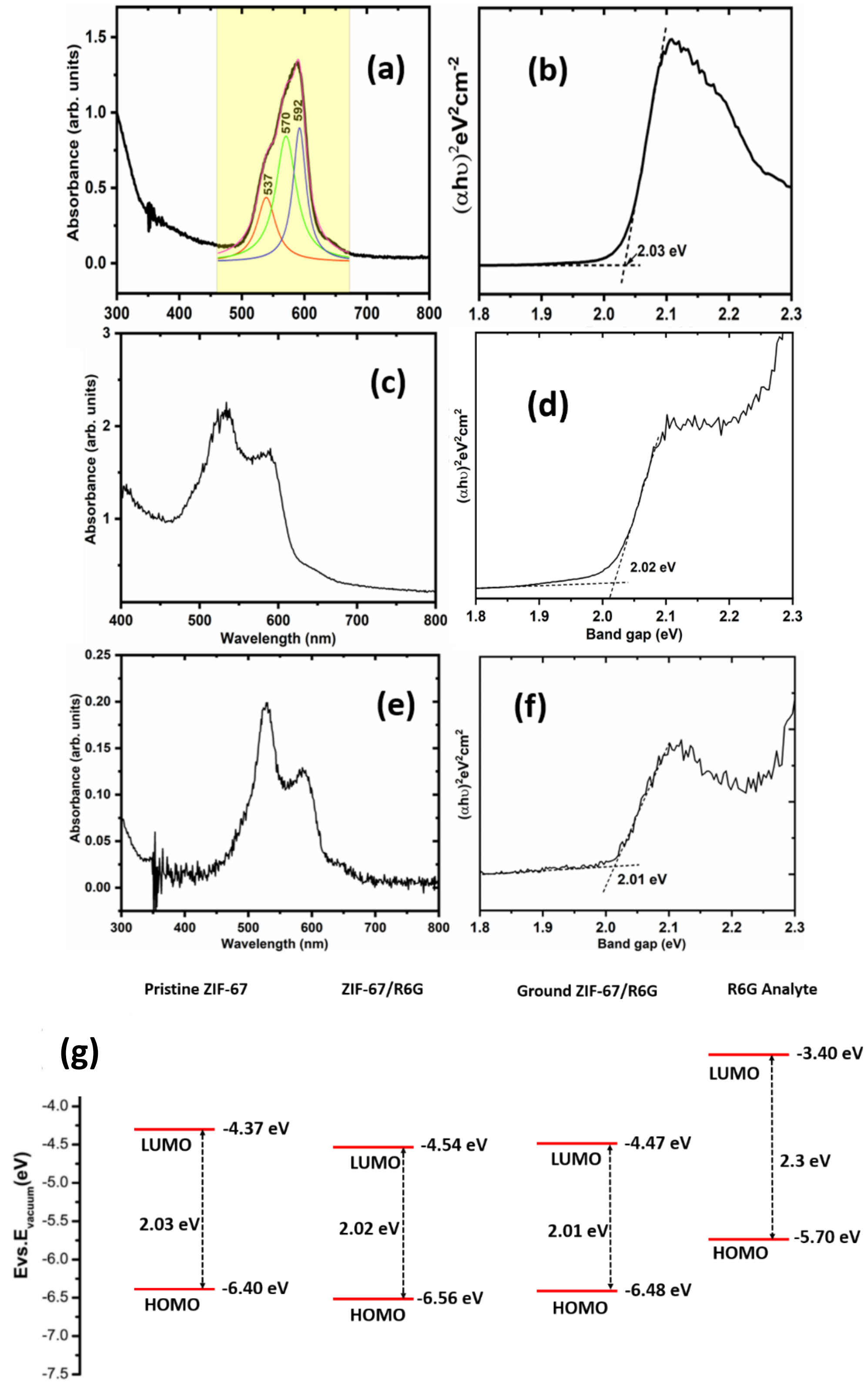

Figure S8 (a-f) UV–vis absorption spectra and the corresponding Tauc plots of ZIF-67, ZIF-67/R6G and hand-ground ZIF-67/R6G. The estimated band gap is indicated in the Tauc plots. (g) Comparison of HOMO and LUMO energy levels of ZIF-67, ZIF-67/R6G and hand-ground ZIF-67/R6G with analyte R6G molecule.

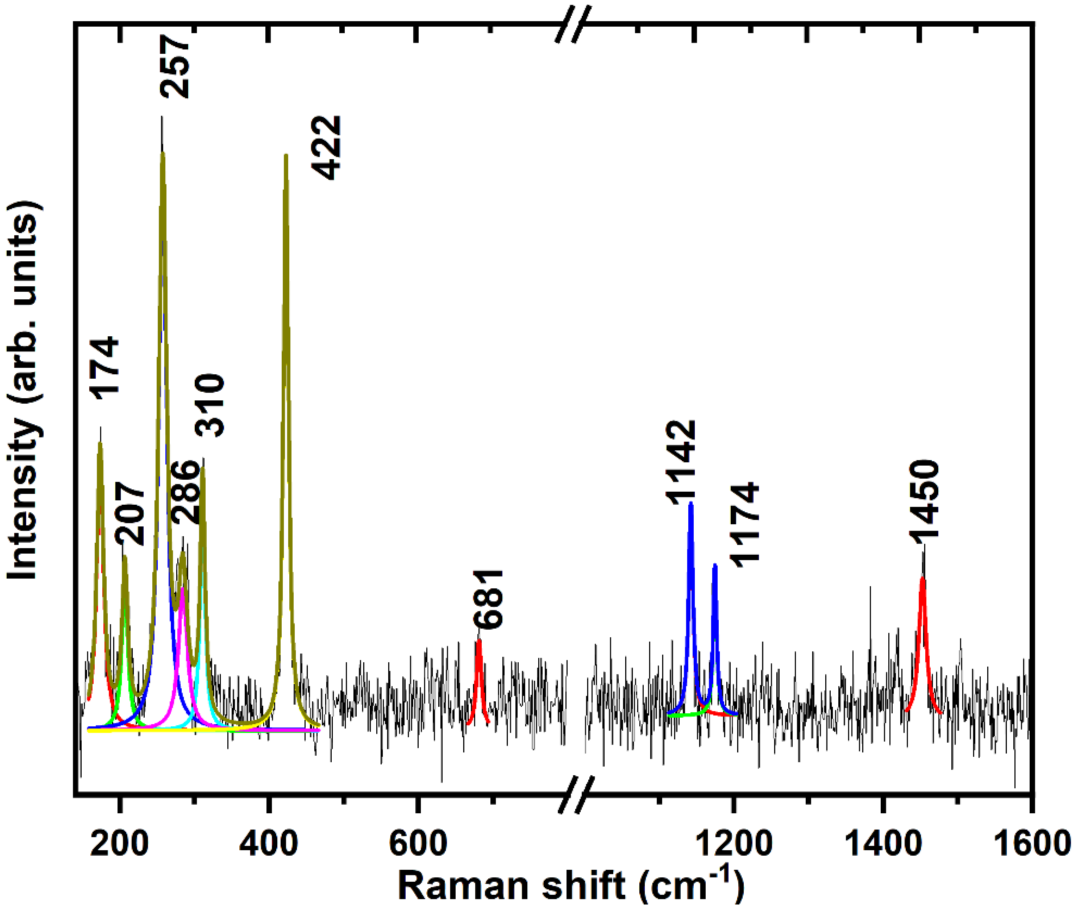

Figure S9. Raman spectrum of pristine ZIF-67 recorded at ambient conditions. The coloured peaks represent the Lorentzian profile fit to the experimentally observed peaks. The peak positions obtained from the fit are indicated in the figure.

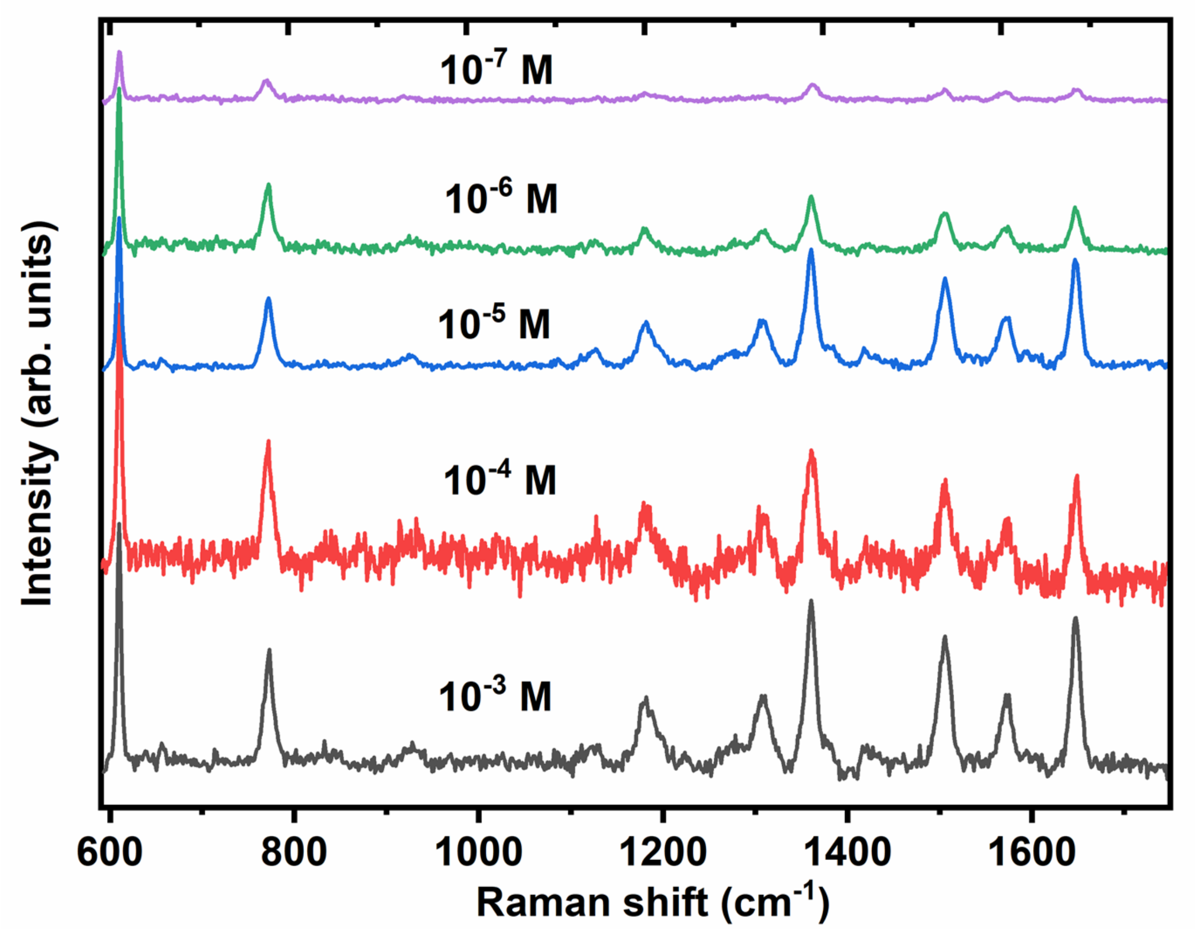

Figure S10. SERS spectra of R6G on the ZIF-67 substrate at different concentrations, 10^{-3}, 10^{-5}, 10^{-6} and 10^{-7} M, suggesting that the detection limit is as low as 10^{-7} M.

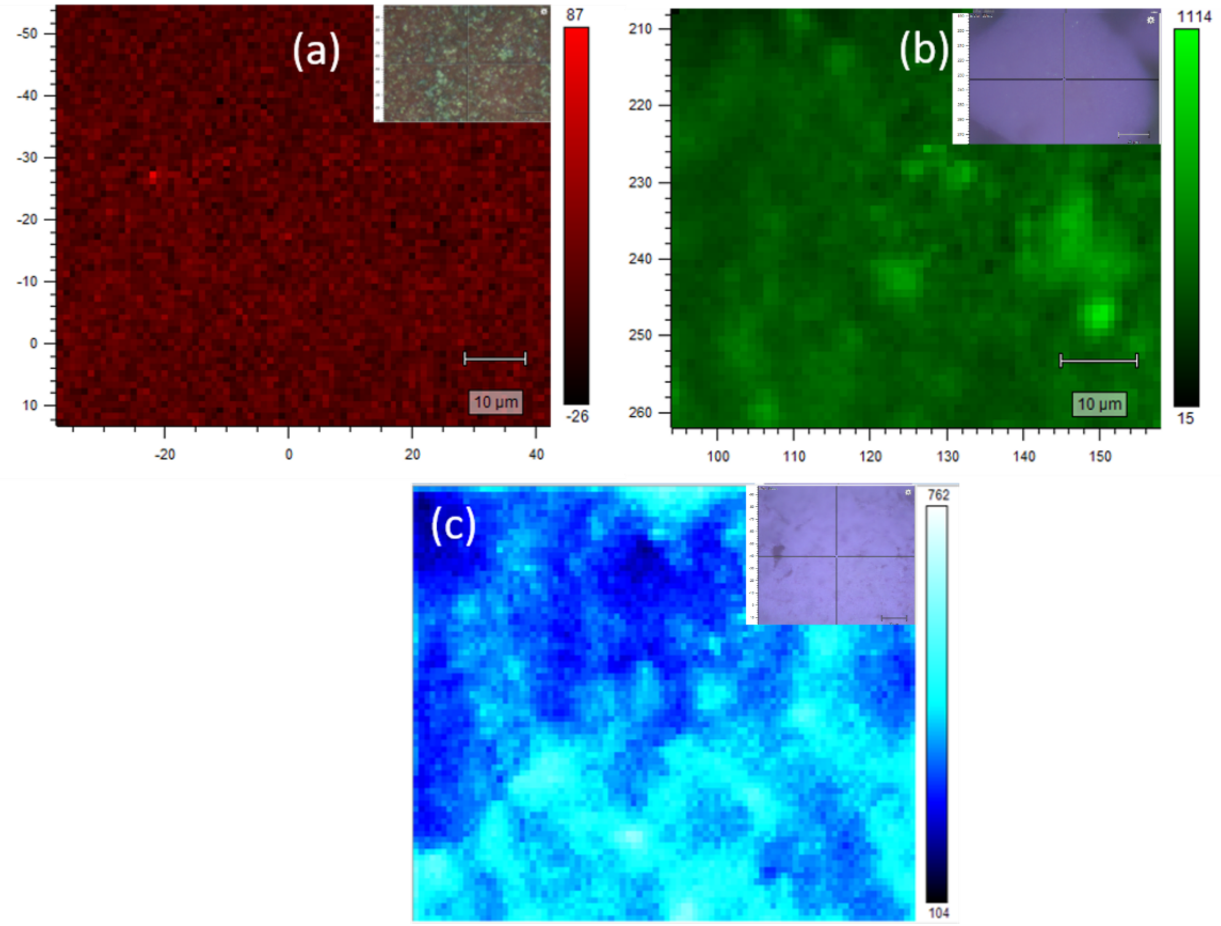

Figure S11. Raman mapping of 612 cm^{-1} peak intensity of R6G analyte molecule of concentration 10^{-3} M on the bare SiO_2/Si (a), ZIF-67 (b) and hand-ground ZIF-67 substrates (c). Inset show the optical microscope images of 10^{-3} M R6G analyte molecules on the above-mentioned substrates.

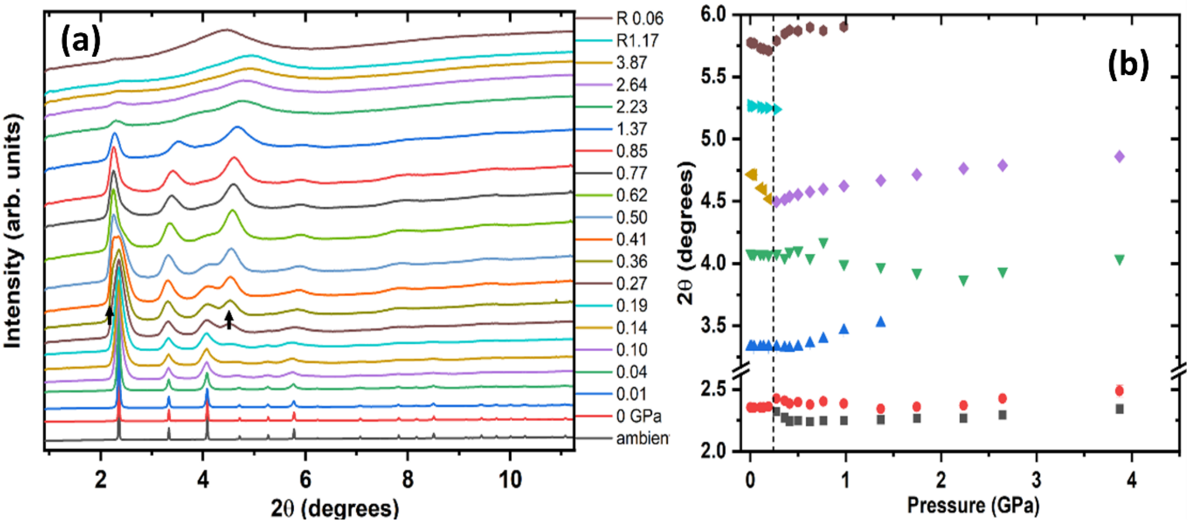

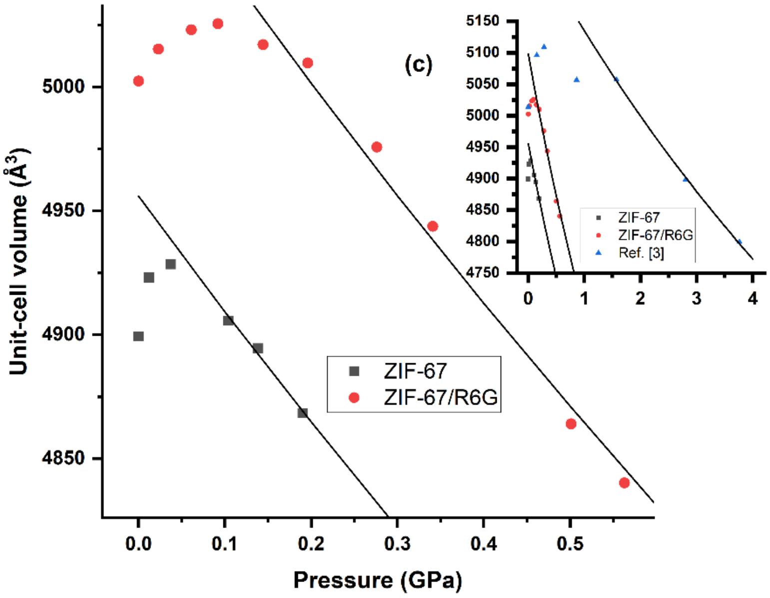

Figure S12. XRPD patterns of ZIF-67 at various pressures on the compression and decompression (the data obtained during the reverse pressure cycle is represented by a prefix R). Arrows indicate the appearance of new reflections (b) Pressure dependence of the Bragg reflection positions (in 2θ) of ZIF-67 on compression in the pressure range of 0–3.84 GPa. (c) Comparison of the unit-cell volume compression of the ZIF-67 and ZIF-67/R6G. Inset here compares the same with that of ZIF-67 with 4:1 methanol-ethanol pressure transmitting medium from Ref [3]. In all the cases, the solid lines are our equation of state fit using second order BM equation. The bulk modulus for the first two cases ~10 GPa whereas it is ~32 GPa in the third case. For the pristine ZIF-67, the unit-cell volume is found to increase until 0.05 GPa. For the ZIF-67/R6G, such an expansion is found to till 0.1 GPa (see also Fig. 3(c) in the main text). The initial increase in the unit-cell volume of the pristine ZIF-67 within the very small pressure range (0.05 GPa) may be due to the insertion of the adsorbed gases inside the pores. In case of ZIF-67/R6G, small pressures may lead to a strong interaction of the R6G molecule with the pores of ZIF-67, leading to a unit-cell volume expansion for pressures up to 0.1 GPa (Fig. 3(c)). However, in both cases, the pore fillings are not sufficient to prevent the system from the pressure induced collapse, unlike the penetrating PTM as reported in Ref. [3].

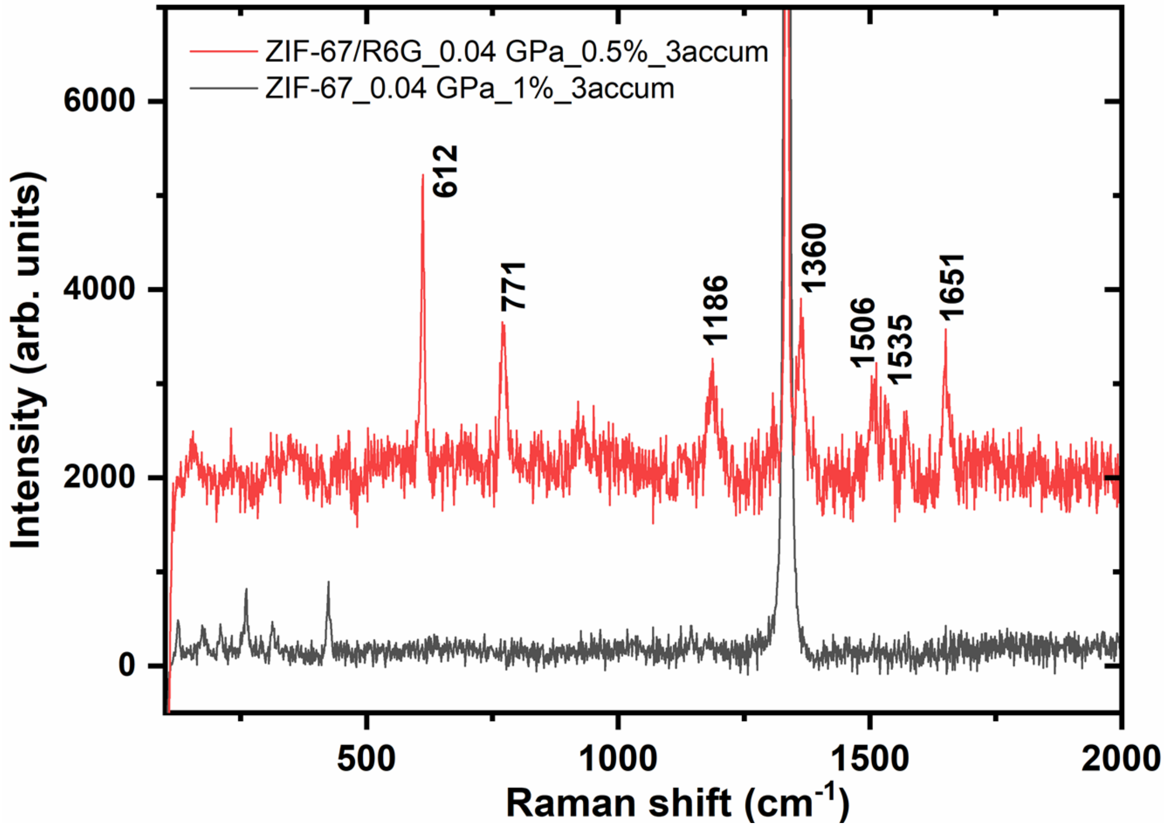

Figure S13. Raman spectrum of pristine ZIF-67 at 0.04 GPa (in black colour) and SERS of ZIF-67/R6G at 0.04 GPa (in red colour). Raman peaks corresponding to R6G are clearly visible. Numbers close to the peaks indicate the mode positions in cm^{-1}. The Raman modes correspond to the ZIF-67 below 500 cm^{-1} are not distinguishable in this condition. The intense peak around 1300 cm^{-1} in both the spectra is from the top diamond of the DAC.

Reference

1 H. Sun, S. Cong, Z. Zheng, Z. Wang, Z. Chen, and Z. Zhao *J. Am. Chem. Soc.***2019**, 141, 870−878.

2 P. Lotti, S. Milani, M. Merlini, B. Joseph, F. Alabarse, A. Lausi, J. Synchrotron Radiation, **2020**, 27, 222−229. https://doi.org/10.1107/S1600577519015170

3 I. M. Jones, et al., CrystEngComm. **2023**, 25, 6533. https://doi.org/10.1039/d3ce00979c